

# Ab initio study of ethylene insertion into M–C bonds of alkylamidinate complexes of group IV ( $\{R'NCRNR'\}_2MCH_3^+$ , M = Zr, Ti, R = H, Ph and R' = H, SiMe<sub>3</sub>)

J. Ramos<sup>a</sup>, V. Cruz<sup>b</sup>, A. Muñoz-Escalona<sup>c</sup>, J. Martínez-Salazar<sup>a,\*</sup>

<sup>a</sup>*GIDEM, Instituto de Estructura de la Materia, CSIC Serrano 119, 28006 Madrid, Spain*

<sup>b</sup>*CTI, CSIC Pinar 19, 28006 Madrid, Spain*

<sup>c</sup>*Repsol I + D, Embajadores 183, 28045 Madrid, Spain*

Received 18 July 2000; received in revised form 21 January 2001; accepted 19 February 2001

## Abstract

Alkylamidinate complexes have been recently reported to be useful catalysts for olefin polymerisation as an alternative to metallocene systems. The present work reports theoretical calculations performed at DFT level for ethylene insertion reactions in zirconium and titanium alkylamidinate compounds with variable structural complexity. The energy barriers obtained for these reactions show that these systems can be considered as efficient olefin polymerisation catalysts, but less active than their metallocene counterparts, in agreement with experimental findings. A comparison between alkylamidinates of Ti and Zr is also provided. © 2001 Elsevier Science Ltd. All rights reserved.

**Keywords:** Poly(ethylene); Homogeneous catalysis; DFT calculations

## 1. Introduction

Metallocenes catalysts have been used for more than 15 years in the polyolefin production and as a consequence they have been widely studied from both experimental [1–3] and theoretical [4–11] points of view. The interest in the development of new catalysts for the olefin polymerisation as alternatives to traditional metallocene catalysts  $Cp_2MR_2$  (where M = Ti, Zr or Hf and R = alkyl or halogen group) has been growing during the last few years. New catalysts based on transition metals containing non-cyclopentadienyl ligands have been developed by several authors. Some examples are titanium and zirconium chelating dialkoxide [12,13], chelating diamido [14–20], boratabenzene [21,22] and benzamidinate [23–31] complexes.

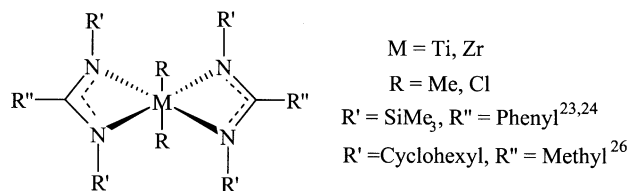
Due to their ease of preparation the group IV benzamidinate complexes have recently received major attention as precursors of transition metal complexes. An important aspect of titanium and zirconium benzamidinate complexes is their potential behaviour as olefin polymerisation catalysts [23–28]. In particular the titanium and zirconium *N,N'*-bis(trimethylsilyl)benzamidinates have been widely explored [23,24]. The metal *N,N'*-bis(trimethylsilyl)benzamidinate complexes would present substantially

different steric and electronic properties at the metal centre as compared to the metal cyclopentadienyl complexes. Wedler et al. [32] compared the benzamidinate ligand to the cyclopentadienyl ligand attached to the same transition metals. By a steric interaction analysis they suggested that the benzamidinate ligand system have a behaviour between the Cp and Cp\* ligands. However, the electronic differences are considerable. The *N,N'*-bis(trimethylsilyl)benzamidinate anions are four-electron donors with two coordination sites whereas the cyclopentadienyl anions are six-electron donating agents with three coordination sites suggesting that electrophilic character of metal centre in complexes of the former anions must increase with respect to the metallocene complexes [23,24].

It has been found experimentally that the zirconium benzamidinate complexes present higher activity for ethylene polymerisation [24] than the titanium counterparts. However, the analogous metallocene catalysts have greater activity for the polymerisation of ethylene [23,24] than the benzamidinate complexes. Eisen et al. have explained the difference in the catalytic activity as a function of the structural environment of the metal centre [23]. They have proposed that the two bulky SiMe<sub>3</sub> group hinder the side approach of ethylene to the catalyst.

Littke et al. [26] have studied other similar catalysts, the bulky bis(alkylamidinate) complexes of group IV. These

\* Corresponding author.



Scheme 1.

complexes are active in the polymerisation of ethylene. In that study, the activity of zirconium complex was found higher than that of the titanium complex. The same trend was found for metallocene and bis(benzamidinate) complexes. The activity of bulky bis(alkylamidinate) was comparable to the bis(benzamidinate) compounds but both present lower activity than analogous metallocene systems. Typical activities for benzamidinate [23,24] and alkylamidinate [26] complexes are around  $10^4$  g polymer/(mol of M)/(atm of ethylene)/h while for metallocene catalysts [1] activities are in the order of  $10^6$  g polymer/(mol of M)/(atm of ethylene)/h.

The general structures of the benzamidinate and alkylamidinate complexes used in polymerisation are depicted in Scheme 1.

Some theoretical studies with non-cyclopentadienyl transition metal complexes for olefin polymerisation have recently been reported [33–44]. However none of them are related to the benzamidinate complexes. The objective of the present investigation is to provide reasonable explanations for the above experimental facts and compare them with similar metallocene systems.

## 2. Computational methods and models used

Experimentally determined structures were extracted from the Cambridge Structural Database [45] and used to build the input geometries for calculations by performing the required changes (i.e. formation of the cationic species, formation of  $\pi$ -complexes and so on).

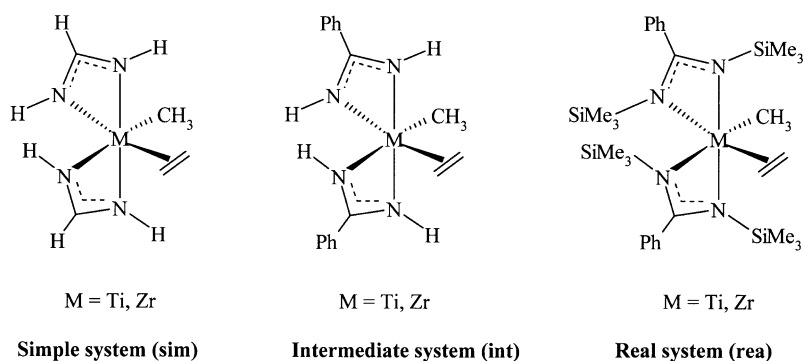
All geometries and structures have been obtained using the Amsterdam Density Functional package (ADF Release

1999.02) [46–48]. The basis set used in all calculations was the II/large-core included in ADF. This basis set does not contain polarisation functions. The valence electronic configurations were described by a double-zeta basis set on all atoms. The inner shells were treated with the frozen core approximation. A set of auxiliary s, p, d, f and g STO functions, centred on all nuclei, was used to fit the molecular density and present Coulomb and exchange potential accurately in each SCF cycle [44,48]. This basis set is comparable to LANL2DZ basis set [49–51].

The calculations have been performed at the local density approximation (LDA) level with the exchange-correlation functional by VWN (Vosko–Wilk–Nusair) [52] augmented by gradient non-local corrections to the exchange and correlation potentials due to Becke [53] and Perdew [54], respectively. These corrections have been included in a perturbative fashion (non-selfconsistent) following convergence on the local density model in such a way that the computing efforts are significantly decreased. Hehre and Lou [55] have compared the manner in which non-local corrections are introduced (in SCF or non-SCF fashion). They found that the geometries and energies appear to be insensitive to the manner in which non-local corrections are introduced.

Since the Cossee–Arman [56] and Brookhart–Green [57] mechanisms are the most accepted for the olefin polymerisation by transition metal catalysts, the key steps of these mechanisms will be used here for the study of titanium and zirconium amidinate complexes. For example, it is well known that the catalytic activity of titanocenes and zirconocenes is associated with the formation of cationic species ( $\text{Cp}_2\text{MR}^+$  where  $M = \text{Ti, Zr}$  and  $R = \text{alkyl chain}$ ). Some authors have also proposed that the active species in titanium and zirconium benzamidinate are cationic alkyl species too [23,28].

Scheme 2 shows the different systems studied. The nomenclature used here is a combination of three different fields: The most simple structures have been labelled as *sim.*, the intermediate as *int.* and the real system as *rea.* The zirconium complexes are referred as 1 and titanium complexes as 2. The  $\pi$ -complexes were labelled as *a*, the transition structures as *b* and the products as *c*. For example,



Scheme 2.

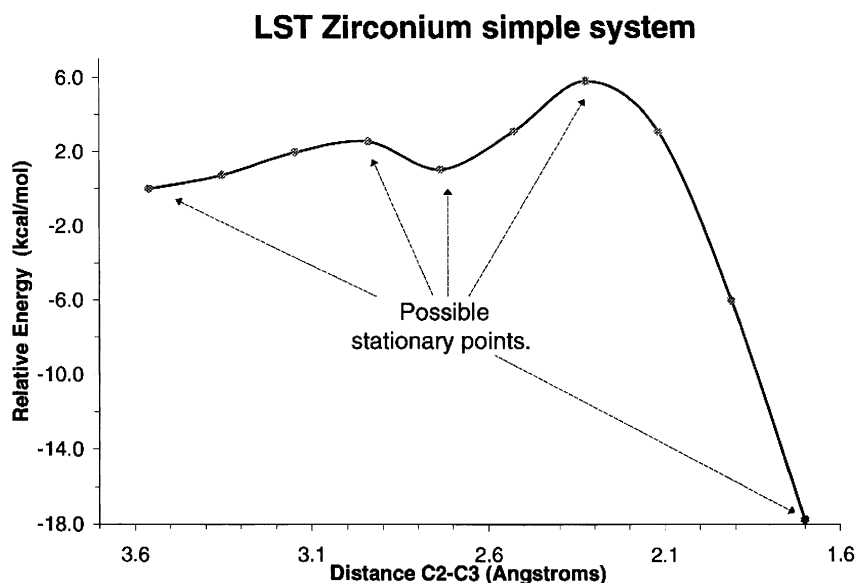


Fig. 1. The linear synchronous transit (LST) path for the ethylene insertion into the zirconium simple system. The distance between the alkyl C atom bonded to the metal centre (C3) and one ethylene C atom (C2) was used as the reaction coordinate.

rea.1b refers to the zirconium transition state structure for the real system.

The approximate reaction paths for the simple systems were obtained by a linear synchronous transit (LST) calculation. The distance between the alkyl C atom bonded to the metal centre and one ethylene C atom was used as the reaction coordinate. The stationary points found along the path were fully optimised either to minima or transition state geometries. The transition state structures found were confirmed by subsequent frequency calculations. The optimised structures for these simple systems were used to build the corresponding structures for the intermediate and real systems. These were afterwards optimised to minimum or transition state geometries.

### 3. Results

This section will be divided in three subsections: simple, intermediate and real amidinate complexes, as mentioned before.

#### 3.1. Zr and Ti simple amidinate systems

The LST path for the ethylene insertion into the zirconium simple system is shown in Fig. 1. As it can be seen, there are five possible stationary points over the LST path. In order to find the true stationary points over the potential energy surface (PES), we performed geometry and transition structure optimisations with the possible candidates. The optimisation and frequency calculation for the step 4 shows that this point is not a true transition state because the vibrational mode corresponding with imaginary frequencies does not connect the expected reactants and products. The same method was used for the titanium simple amidinate

system and equivalent stationary points were obtained (the LST for titanium is not shown here for simplicity). A remarkable aspect of these LST paths is the fact that the coordination around metal centre changes at the insertion product (see below).

The structures and energies for the optimised stationary points are displayed in Fig. 2 and Table 1, respectively.

The two amidinate ligands constitute two mutually perpendicular four-membered rings with the metal atom as the joining point between these planes. The angle between these planes is called the Benz-Ang (benzamidinate angle, see Scheme 3). This angle gives an idea of the relative orientation of the two amidinate ligands. The Benz-Ang in conjunction with the  $N1-M-N1'$  angle will give a picture of the coordination around the metal centre (for definitions of these angles see Scheme 3).

Two ethylene  $\pi$ -complexes (sim.1a and sim.1a') were found for zirconium simple systems. The main difference between them is the placement of the ethylene monomer

Table 1

Relative energies for the (a) reactants, (b) transition structures and (c) direct insertion products of simple amidinate zirconium and titanium models. The nomenclature is described in Section 2 and in Fig. 2. Energies are in kcal/mol

Simple amidinate zirconium		Simple amidinate titanium	
Compounds	$E_{\text{relative}}^a$	Compounds	$E_{\text{relative}}^a$
sim.1a'	-0.86	sim.2a'	-0.88
sim.1a	0.00	sim.2a	0.00
sim.1b	+4.54	sim.2b	+6.31
sim.1c	-23.17	sim.2c	-23.10

<sup>a</sup> Energies are relative to the so-called parallel  $\pi$ -complex (sim.1a or sim.2a), for both zirconium and titanium systems.

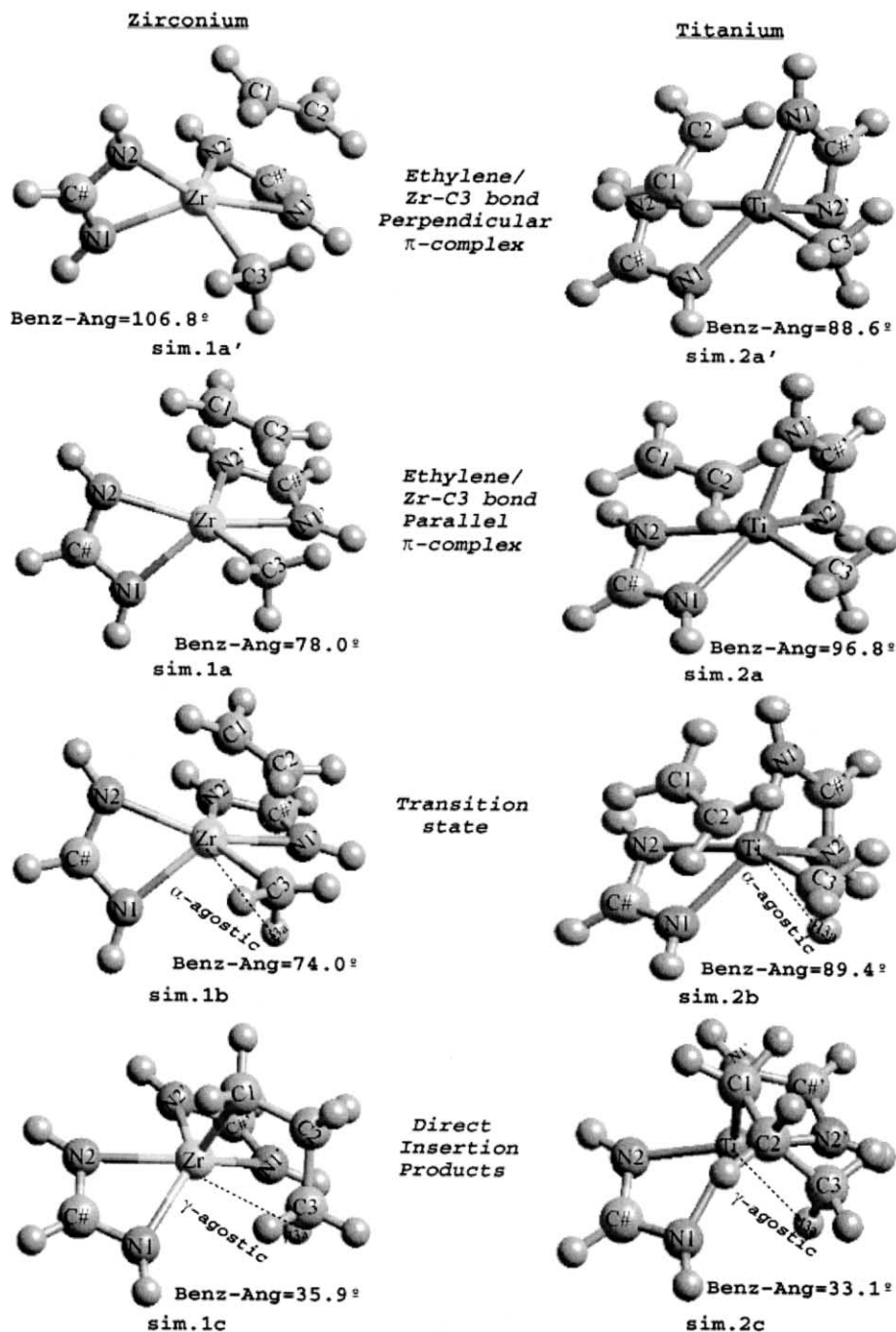


Fig. 2. Structures for all stationary points for ethylene insertion into the zirconium and titanium simple systems.

with respect to the Zr–C3 bond. In sim.1a the ethylene is placed parallel to the Zr–C3 bond whereas in sim.1a' the ethylene is in a perpendicular position. The perpendicular  $\pi$ -complex is slightly more stable than the parallel one (–0.86 kcal/mol for zirconium, see Table 1). The same results are found for the Ti complexes, sim.2a and sim.2a' (–0.88 kcal/mol for titanium, see Table 1). Therefore, the precursor corresponding to the insertion of ethylene into the M–C bond could be the parallel form. As it was indicated above, the transition state between the two  $\pi$ -complexes

(sim.a and sim.a') was not found, so the energy barrier between the perpendicular and parallel conformations is expected to be very small. The geometries for the zirconium and titanium complexes are very similar for both perpendicular and parallel forms.

The transition states corresponding to the ethylene insertion were optimised for the zirconium (sim.1b) and titanium (sim.2b) simple complexes. Both transition structures were confirmed by frequency calculations ( $\nu_{\text{im}} = -200 \text{ cm}^{-1}$  for Zr and  $\nu_{\text{im}} = -162 \text{ cm}^{-1}$  for titanium) with additional

animation of their imaginary vibrational modes to check whether these transition structures correspond to those expected. For the zirconium system the energy of the transition structure sim.1b is 4.54 kcal/mol above the parallel  $\pi$ -complex sim.1a, while in the case of the titanium complex the energy is 6.31 kcal/mol. This result is in agreement with the experimental results where the zirconium amidinates are found to be more active for the ethylene polymerisation than the titanium amidinates [24]. The same tendency has been found for the Zr and Ti metallocene systems. The geometries of the transition states (sim.1b and sim.2b) of these simple amidinates systems present  $\alpha$ -agostic interactions ( $\text{Zr-H}\alpha = 2.37\text{\AA}$   $\text{Ti-H}\alpha = 2.21\text{\AA}$ ) since both the metal and the four atoms involved in the reaction (M, C1, C2, C3) are practically placed in the same plane as showed by the dihedral angles  $\text{C3-Zr-C1-C2}$  ( $14.3^\circ$ ) and  $\text{C3-Ti-C2-C1}$  ( $-9.4^\circ$ ) (as can be seen in Fig. 2), in agreement with the Brookhart–Green mechanism [57].

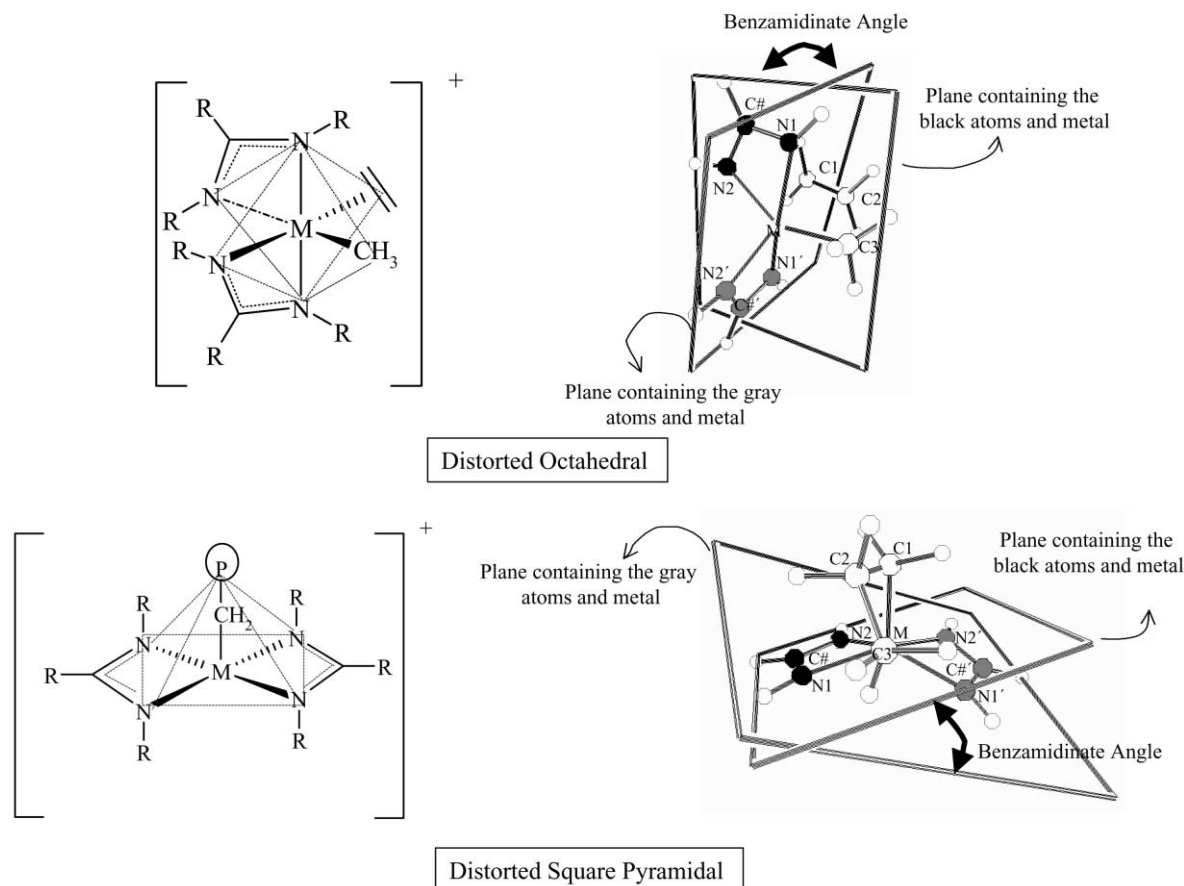
The direct insertion products for the zirconium and titanium have been optimised. A remarkable fact is that coordination around the metal centre changes from distorted octahedral in the reactants ( $\text{N1-Zr-N1}' = 159.5^\circ$  and  $\text{Benz-Ang} = 78.0^\circ$  for zirconium and  $\text{N1-Ti-N1}' = 156.8^\circ$  and  $\text{Benz-Ang} = 96.8^\circ$  for titanium) to distorted square pyramidal in the products ( $\text{N1-Zr-N1}' = 128.3^\circ$  and  $\text{Benz-Ang} = 35.9^\circ$  for zirconium and  $\text{N1-Ti-N1}' = -127.8^\circ$  and  $\text{Benz-Ang} = 33.1^\circ$  for titanium, see Fig. 2). Geometry optimisation with distorted octahedral coordination have been tried for the simple amidinate zirconium product, but it converges to the structures with a distorted square-planar-pyramid coordination. It was then concluded that this coordination change between reactants and products during the insertion reaction is not possible in real systems due to the presence of bulky  $\text{SiMe}_3$  groups attached to the nitrogen atoms which would hinder the rotation of amidinate ligands (as it will be shown below).

Geometry optimisation with distorted octahedral coordination have been tried for the simple amidinate zirconium product, but it converges to the structures with a distorted square-planar-pyramid coordination. It was then concluded that this coordination change between reactants and products during the insertion reaction is not possible in real systems due to the presence of bulky  $\text{SiMe}_3$  groups attached to the nitrogen atoms which would hinder the rotation of amidinate ligands (as it will be shown below).

### 3.2. Zr and Ti intermediate benzamidinates ligands

The intermediate benzamidinate system is depicted in Scheme 2. The complete structures are not shown here, as they are similar to those exhibited by the simple model system. Only the main differences observed relative to the simple model structures are reported.

The phenyl group positions define the principal characteristic of the intermediate systems. The  $\text{N1-C\#-C}^*-\text{C}^*$  angle gives an idea of the position of the phenyl group with respect to the amidinate ligand (see Fig. 3). In the geometry found experimentally [14,15], the phenyl groups are placed perpendicular to the amidinates planes. However, after



Scheme 3.

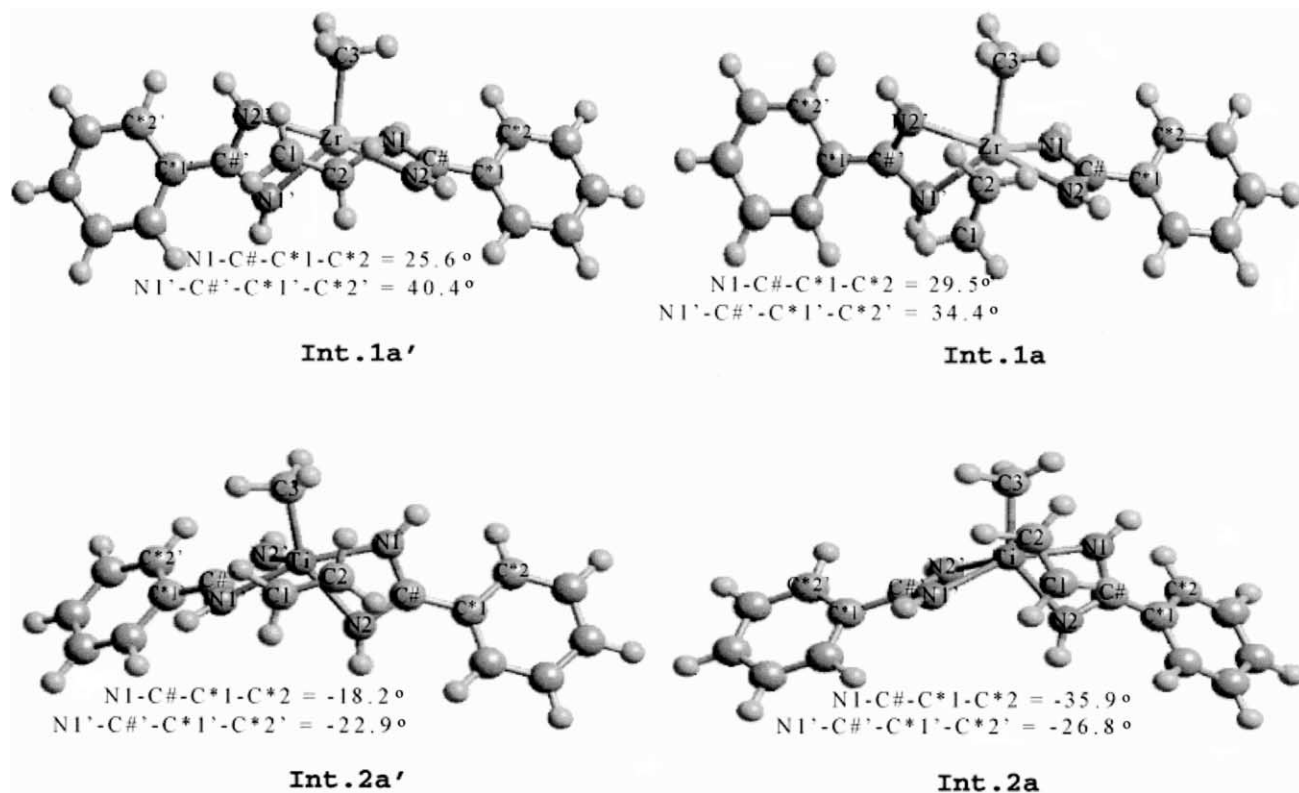


Fig. 3. Ethylene  $\pi$ -complexes for the zirconium and titanium intermediate systems. The angles shown here give an idea of the relative position of the phenyl group with respect to the amidinate ligand.

optimisation these phenyl groups are placed near coplanar to the amidinate planes (see  $\text{NI}-\text{C}\#-\text{C}^*-\text{C}^*$  angle in Fig. 3), suggesting a possible conjugation between the phenyl and the amidinate ligands (Fig. 3). The phenyl groups tend to be more coplanar with the amidinate planes in the titanium complex than in the zirconium complex (compare, for instance,  $\text{int.1a}'$  with  $\text{int.2a}'$ , in Fig. 3).

The computed energies for the intermediate models are shown in Table 2. Similar to the simple model, the perpendicular  $\pi$ -complex appears to be more stable than the

parallel  $\pi$ -complex for both metals. However the stability of the perpendicular form is more remarkable for the titanium complex ( $-3.65$  kcal/mol) relative to the zirconium one ( $-0.78$  kcal/mol), suggesting a possible stabilisation due to greater conjugation between phenyl groups and the amidinate ligands in the titanium ( $\text{int.2a}'$ ) complex with respect to the zirconium systems ( $\text{int.1a}'$ ).

The energy barrier for the ethylene insertion into the intermediate titanium system is lower than for the intermediate zirconium one ( $+4.95$  kcal/mol versus  $+5.36$  kcal/mol, see Table 2), suggesting a higher activity for the titanium complexes as compared to the zirconium ones. This tendency is opposite to that observed for the simple system (see above) and also to the experimental activity reported for the benzamidinate complexes of titanium and zirconium [27,29]. However, the energy difference is very small (lower than  $0.41$  kcal/mol) so it is expected that any experimental factor not considered here (solvent, cocatalyst, etc.) could reverse this tendency.

Furthermore it has been observed for the intermediate systems the same coordination change in the products with respect to the reactants. This coordination change could be due again to the lower steric interactions in the distorted square pyramidal with respect to the complex with distorted octahedral coordination, as it was postulated for the simple system.

Table 2

Relative energies for the (a) reactants, (b) transition structures and (c) direct insertion products of intermediate amidinate zirconium and titanium models. The nomenclature is described in Section 2 and in Fig. 2. Energies are in kcal/mol

Intermediate amidinate zirconium		Intermediate amidinate titanium	
Compounds	$E_{\text{relative}}^a$	Compounds	$E_{\text{relative}}^a$
$\text{int.1a}'$	-0.78	$\text{int.2a}'$	-3.65
$\text{int.1a}$	0.00	$\text{int.2a}$	0.00
$\text{int.1b}$	+5.36	$\text{int.2b}$	+4.95
$\text{int.1c}$	-20.70	$\text{int.2c}$	-20.58

<sup>a</sup> Energies are relative to the so-called parallel  $\pi$ -complex ( $\text{int.1a}$  or  $\text{int.2a}$ ) for both zirconium and titanium intermediate systems.

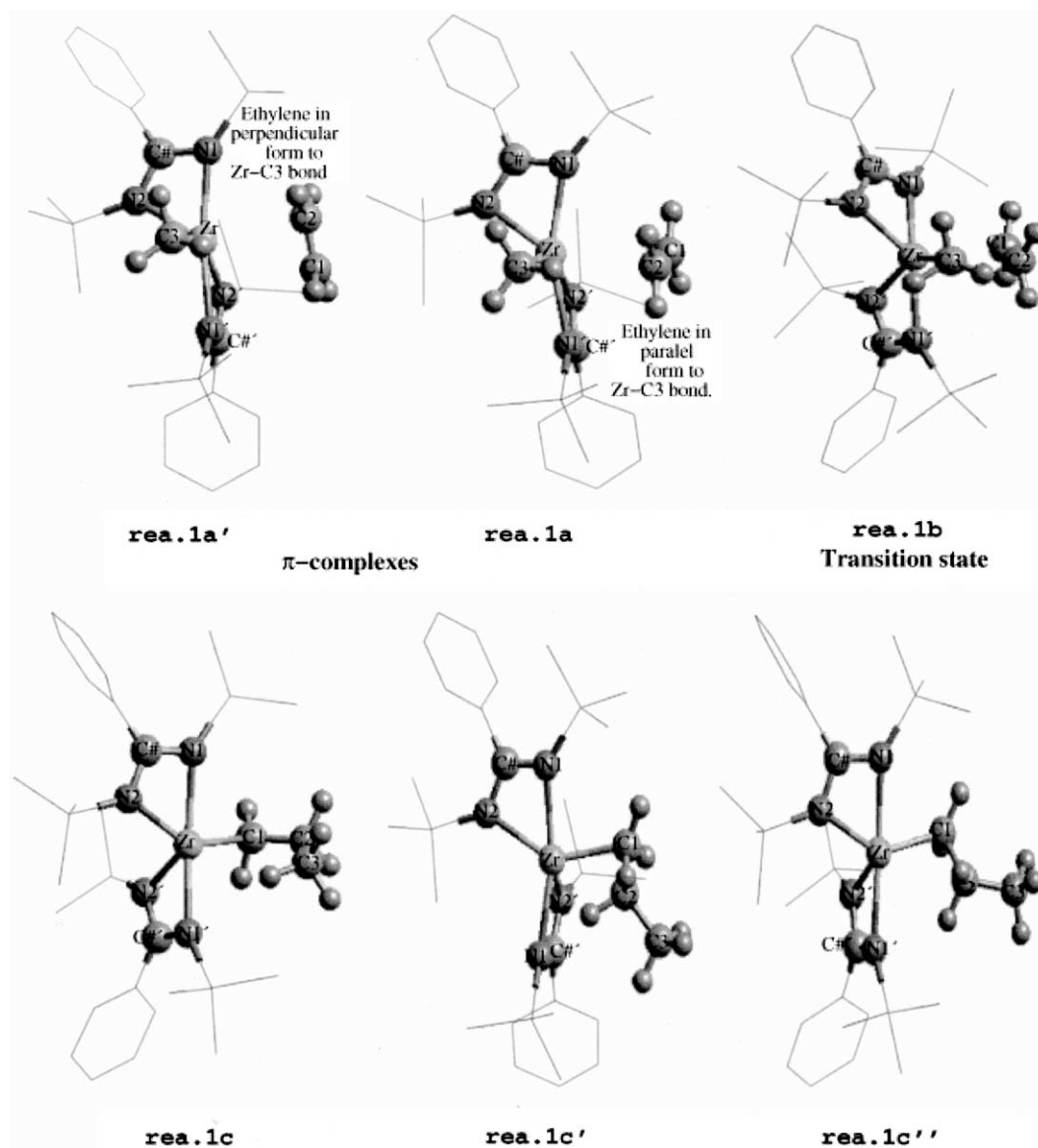


Fig. 4. Structures for all stationary points found for the ethylene insertion into  $N,N'$ -bis(trimethylsilyl)benzamidates zirconium. For clarity the hydrogens for the Ph and  $\text{SiMe}_3$  groups are not shown.

### 3.3. Zr and Ti real $N,N'$ -bis(trimethylsilyl)benzamidinate ligands

Real amidinate ligands correspond to the  $N,N'$ -bis(trimethylsilyl)benzamidinate complexes that have been recently synthesised [23–25,27] (see Schemes 1 and 2). These titanium and zirconium complexes showed similar catalytic activity for the olefin polymerisation, but lower than the metallocene complexes [24].

Geometry optimisation of the  $\text{L}_2\text{Zr}(\text{CH}_3)_2$  system (where L is  $N,N'$ -trimethylsilylbenzamidinate) was performed in order to compare with the experimental structures [23–25,27]. The molecular geometries obtained with the DFT-BP86/II model (see Section 2) reproduce the experimental structures within an error of 0.1 Å for bond distances and  $2.0^\circ$  for bond and torsion angles. Previous calculations at

RHF/LANL2DZ level and PM3(tm) semiempirical model were not able to reproduce the experimental geometry.

Stationary points on the potential energy surface (PES) for zirconium benzamidates were found and they are displayed in Fig. 4. Geometrical parameters and energies are shown in Table 3. For the titanium benzamidates the stationary points are not shown for simplicity. However, geometrical parameters and energies are shown in Table 4.

The geometry of the metal centre corresponds to a distorted octahedral (see  $\text{N1-M-N1}'$  angle and Benz-Ang in Tables 3 and 4) with four nitrogen atoms, a methyl ligand and an ethylene monomer forming the coordination sphere. The methyl and the ethylene monomer are in *cis* position in the octahedral structure. The phenyl groups remain almost perpendicular with respect to the four-member rings (see  $\text{N1-C\#-C* -C*}$  torsion Tables 3 and 4), excluding the

Table 3

Selected geometry parameters and energies for all the stationary points found during the ethylene insertion into Zr–C bond of zirconium benzamidinate complexes (real amidinate systems). The nomenclature is described in the Section 2 and in Fig. 4. Energies in kcal/mol, distances in angstroms and angles in degrees. The M–H distances in bold type indicate the agostic interaction

$E_{\text{relative}}^a$	rea.1a'	rea.1a	rea.1b	rea.1c	rea.1c'	rea.1c''
	+1.15	0.00	+10.32	−4.02	−7.60	−7.70
Zr–C1	2.917	2.810	2.396	2.275	2.238	2.264
Zr–C2	2.624	2.738	2.686	3.267	2.672	3.254
Zr–C3	2.241	2.236	2.308	3.234	3.876	3.191
C1–C2	1.349	1.346	1.387	1.536	1.521	1.533
C2–C3	3.216	3.685	2.251	1.544	1.546	1.525
Zr–H1a <sup>b</sup>	–	–	–	2.540	2.759	<b>2.539</b>
Zr–H1b <sup>b</sup>	–	–	–	2.978	2.981	2.960
Zr–H2a <sup>c</sup>	–	–	–	3.870	<b>2.246</b>	3.853
Zr–H2b <sup>c</sup>	–	–	–	4.138	3.294	4.122
Zr–H3a <sup>d</sup>	2.948	2.933	<b>2.428</b>	<b>2.456</b>	4.095	2.771
Zr–H3b <sup>d</sup>	2.689	2.697	3.299	4.053	4.783	4.261
Zr–H3c <sup>d</sup>	2.807	2.813	2.642	3.736	4.163	3.142
Zr–C1–C2	88.4	73.0	86.1	116.7	88.5	116.6
C1–C2–C3	–	–	116.5	112.3	116.6	111.0
C#–Zr–C#'	140.1	138.4	132.8	137.3	136.2	136.7
N1–Zr–N1'	165.1	163.8	151.9	165.4	163.1	165.9
Zr–C1–C2–C3	36.0	−1.3	−11.9	15.4	124.1	17.0
C3–Zr–C1–C2	−72.9	1.7	10.4	–	–	–
N1–C#–C*–C*	110.8	111.8	83.3	75.8	75.8	75.9
N1'–C#–C*–C*'	110.0	108.1	70.3	72.2	74.7	78.9
Benz-Ang <sup>e</sup>	113.3	108.0	106.7	105.7	102.2	106.1

<sup>a</sup> Energies are relative to rea.1a.

<sup>b</sup> Hydrogen attached to C1.

<sup>c</sup> Hydrogen attached to C2.

<sup>d</sup> Hydrogen attached to C3.

<sup>e</sup> Angle between N1C#N2Zr plane and N1'C#N2'Zr plane.

conjugation between the aromatic rings and the amidinate groups.

Similarly to simple and intermediate complexes, the incoming ethylene monomer is coordinated with the metal in parallel or perpendicular positions with respect to the M–C bond. The parallel complexes are more stable by about 1 kcal/mol with respect to the perpendicular ones (see Tables 3 and 4). This tendency is opposite to what was found in the simple and intermediate systems probably due to the steric repulsion between the bulky SiMe<sub>3</sub> groups and the ethylene monomer. The parallel form is the precursor  $\pi$ -complex for olefin insertion into the M–C3 bond, in the same way as for metallocene systems [4–11].

In order to find the energy barriers of the ethylene insertion into the benzamidinate complexes, the transition states for the insertion reactions are located. The energy barrier for the ethylene insertion into the titanium benzamidinate complex is 9.67 kcal/mol while for the corresponding zirconium complex it is 10.32 kcal/mol (see Tables 3 and 4). Experimentally, it has been reported that the zirconium benzamidinates show more activity than the titanium benzamidinates for the ethylene polymerisation. There is no agreement between the experiments and the theoretical results. However the difference between energy barriers is very small (lower than 1 kcal/mol). For this reason, addi-

tional factors other than only energy barriers should be taken into account as an explanation of the ordering in activity for these catalysts. It should be mentioned that the energy barriers calculated for the ethylene insertion into the M–C bonds for the benzamidinate complexes are larger compared to that for ethylene insertion into metallocene complexes [4–11] (about 3–7 kcal difference). This observation is consistent with the experimental fact that the metallocene catalysts are more active for ethylene polymerisation than the benzamidinate catalysts. It has been reported that the metallocene complexes are more active than the benzamidinate complexes by about two orders of magnitude [1–3,23,24,28].

The coordination change around the metal centre, discussed above for the simple and the intermediate systems, is not observed in the products of the real model. The benzamidinate planes cannot rotate from the distorted octahedral coordination to the distorted square pyramidal due to the steric hindrance produced by the bulky SiMe<sub>3</sub> groups attached to N atoms in these real systems.

Several products were found for the insertion of ethylene into the metal *N,N'*-bis(trimethylsilyl)benzamidinate complexes (see Fig. 4). The main differences between these products are the type of agostic interaction and the M–C1–C2–C3 dihedral angles of the growing chain.



Table 4

Selected geometry parameters and energies for all the stationary points found during the ethylene insertion into the Ti–C bond of titanium benzamidinate complexes (real amidinate systems). The nomenclature is described in Section 2 and in Fig. 4. Energies are in kcal/mol, the distances in angstroms and the angles in degrees. The M–H distances in bold type indicate the agostic interaction

$E_{\text{relative}}^a$	rea.2a'	rea.2a	rea.2b	rea.2c	rea.2c'
	+0.95	0.00	+9.67	–8.81	–13.64
Ti–C1	2.523	2.652	2.250	2.132	2.593
Ti–C2	2.803	2.534	2.482	3.083	2.095
Ti–C3	2.095	2.096	2.161	3.066	3.797
C1–C2	1.348	1.347	1.390	1.531	1.519
C2–C3	3.480	3.104	2.196	1.548	1.543
Ti–H1a <sup>b</sup>	–	–	–	2.785	2.797
Ti–H1b <sup>b</sup>	–	–	–	2.477	2.625
Ti–H2a <sup>c</sup>	–	–	–	3.867	3.250
Ti–H2b <sup>c</sup>	–	–	–	3.816	<b>2.212</b>
Ti–H3a <sup>d</sup>	2.560	2.788	<b>2.268</b>	<b>2.314</b>	4.126
Ti–H3b <sup>d</sup>	2.672	2.542	2.560	3.657	4.696
Ti–H3c <sup>d</sup>	2.770	2.672	3.125	3.848	3.978
Ti–C1–C2	–	–	–	113.6	90.2
C1–C2–C3	–	–	–	114.1	115.1
C#–Ti–C#'	139.5	140.7	137.2	142.5	140.9
N1–Ti–N1'	166.7	163.3	168.9	162.3	163.5
Ti–C1–C2–C3	35.2	2.6	3.1	3.2	124.4
C3–Ti–C1–C2	–72.6	2.4	–2.7	–1.8	–2.8
N1–C#–C * –C *	118.9	116.2	114.5	100.8	103.5
N1'–C#'/C *'–C *'	109.6	111.7	113.4	103.3	99.6
Benz–Ang <sup>e</sup>	107.9	103.7	103.5	104.7	104.3

<sup>a</sup> Energies are relative to rea.2a.

<sup>b</sup> Hydrogen attached to C1.

<sup>c</sup> Hydrogen attached to C2.

<sup>d</sup> Hydrogen attached to C3.

<sup>e</sup> Angle between N1C#N2Ti plane and N1'C#N2'Ti plane.

For the zirconium complex three structures were found (rea.1c, rea.1c', rea.1c'', see Fig. 4). The product rea.1c is the direct  $\gamma$ -agostic product, rea.1c' is a  $\beta$ -agostic structure while the rea.1c'' presents a small  $\alpha$ -agostic interaction. The rea.1c'' is the most stable product. The product with  $\beta$ -agostic interaction is slightly less stable (rea.1c') than rea.1c'', making a difference to what has been observed in the metallocene systems [2] where the  $\beta$ -agostic structure is always the most stable product. However, the  $\gamma$ -agostic product (rea.1c) is less stable than the  $\beta$ -agostic product (rea.1c) by 3.68 kcal/mol, as occurs in the metallocene catalysts [4–11].

For the titanium complex only two products were obtained, the  $\gamma$ -agostic (rea.2c) and the  $\beta$ -agostic (rea.2c') complexes. The  $\gamma$ -agostic product is also less stable than the  $\beta$ -agostic by 4.83 kcal/mol.

It is known that the  $\gamma$ -agostic structure is the direct insertion product and the  $\beta$ -agostic complex is the precursor of some termination processes [4–11] ( $\beta$ -elimination and  $\beta$ -transfer to the monomer). For the titanium complex the  $\beta$ -agostic structure is relatively more stable with respect to  $\gamma$ -agostic product than in the zirconium complex (4.83 kcal/mol for Ti against 3.68 kcal/mol for Zr). A more stable  $\beta$ -agostic complex

could be the reason for the lower molecular weight polyethylenes found experimentally in the titanium amidinates as compared to the zirconium ones [26].

#### 4. Conclusions

The calculations reported in the present paper show that benzamidinates of Zr and Ti are effective ethylene polymerisation catalysts from the theoretical point of view, and could constitute an acceptable alternative to the metallocene systems, although they seem to be less active than the former.

The energy barriers found for the ethylene insertion reaction into the Zr and Ti benzamidinates are very similar, consequently this magnitude could not explain alone the relative order of activity between both metals.

For the real system, the function of bulky SiMe<sub>3</sub> groups attached to N atoms is twofold: (a) first, it prevents the coordination change from distorted octahedral to distorted square-planar pyramid structure and, (b) secondly, it makes easier the parallel orientation of the incoming ethylene.

The  $\beta$ -agostic product is the precursor of two of the most common chain termination reactions in olefin polymerisation

( $\beta$ -elimination and  $\beta$ -transfer to the monomer). Therefore, the relative stability of this structure could give an explanation of the molecular weight of the polymer. Accordingly, the zirconium benzamidinate complexes could give rise to polymers with higher molecular weights than the corresponding titanium complexes, in agreement with the experimental results.<sup>1</sup>

## Acknowledgements

Thanks are due to the CICYT (Grant MAT99-1053) for the support of this investigation. One of us (J.R.) wishes to thank CICYT for the tenure of a fellowship. The authors also acknowledge Repsol-YPF for the permission to publish these data.

## References

- [1] Soares JBP, Hamielec AE. *Polym React Engng* 1995;117:3008.
- [2] Brintzinger HH, Fischer D, Müllhaupt R, Rieger B, Waymouth RM. *Angew Chem, Int Ed Engl* 1995;34:1143.
- [3] Kaminsky W, Sinn H. *Transition metals and organometallics for catalysts for olefin polymerisation*. New York: Springer, 1988.
- [4] Kawamura-Kuribayashi H, Koga N, Morokuma K. *J Am Chem Soc* 1992;114:8687.
- [5] Meier RJ, Van Doremaele GHJ, Iarlari S, Buda F. *J Am Chem Soc* 1994;116:7274.
- [6] Yoshida T, Koga N, Morokuma K. *Organometallics* 1995;14:746.
- [7] Cruz VL, Muñoz-Escalona A, Martínez-Salazar J. *Polymer* 1996;37:1663.
- [8] Woo TK, Margl PM, Lohrenz JCW, Blöchl PE, Ziegler T. *J Am Chem Soc* 1996;118:13021.
- [9] Cruz VL, Muñoz-Escalona A, Martínez-Salazar J. *J Polym Sci, Part A: Polym Chem* 1998;36:1157.
- [10] Muñoz-Escalona A, Ramos J, Cruz VL, Martínez-Salazar J. *J Polym Sci, Part A: Polym Chem* 2000;38:571.
- [11] Ramos J, Cruz VL, Muñoz-Escalona A, Martínez-Salazar J. *Polymer* 2000;41:6161.
- [12] Mack H, Eisen MS. *J Chem Soc, Dalton Trans* 1998;6:917.
- [13] Van der Linden A, Schaverien CJ, Meijboom N, Ganter C, Orpen AG. *J Am Chem Soc* 1995;117:3008.
- [14] Scollard JD, McConville DH, Payne NC, Vittal JJ. *Macromolecules* 1996;29:5241.
- [15] Mack H, Eisen MS. *J Organomet Chem* 1996;525:81.
- [16] Scollard JD, McConville DH. *J Am Chem Soc* 1996;118:10008.
- [17] Scollard JD, McConville DH, Vittal JJ. *Organometallics* 1997;16:4415.
- [18] Scollard JD, McConville DH, Vittal J, Payne NC. *J Mol Catal A: Chem* 1998;128:201.
- [19] Warren TH, Schrock RR, Davis WM. *Organometallics* 1998;17:308.
- [20] Jeon Y, Park SJ, Heo J, Kim K. *Organometallics* 1998;17:3161.
- [21] Rogers JS, Bazan GC, Sperry CK. *J Am Chem Soc* 1997;119:9305.
- [22] Bazan GC, Rodriguez G, Ashe III AJ, Al-Ahmad S, Kampf JW. *Organometallics* 1997;16:2492.
- [23] Herskovics-Korine D, Eisen MS. *J Organomet Chem* 1995;503:307.
- [24] Flores JC, Chien JCW, Rausch MD. *Organometallics* 1995;14:1827.
- [25] Averbuj C, Tish E, Eisen MS. *J Am Chem Soc* 1998;120:8640.
- [26] Littke A, Sleiman N, Bensiman C, Richeson DS, Yap GPA, Brown SJ. *Organometallics* 1998;17:446.
- [27] Volkis V, Shmulinson M, Averbuj C, Lisovskii A, Edelmann FT, Eisen MS. *Organometallics* 1998;17:3155.
- [28] Gomez R, Green MHL, Haggitt JL. *J Chem Soc, Dalton Trans* 1996;6:939.
- [29] Roesky HW, Meller B, Noltemeyer M, Schmidt HG, Scholz U, Sheldrick GM. *Chem Ber* 1988;121:1403.
- [30] Walther D, Fischer R, Friedich F, Gebhardt P, Görls H. *Chem Ber* 1996;129:1389.
- [31] Hagadorn JR, Arnold J. *J Chem Soc, Dalton Trans* 1997;18:3087.
- [32] Wedler M, Knösel F, Noltemeyer MN, Edelman FT. *J Organomet Chem* 1990;388:21.
- [33] Musaev DG, Froese RDJ, Svensson M, Morokuma K. *J Am Chem Soc* 1997;119:367.
- [34] Musaev DG, Svensson M, Morokuma K, Strömberg S, Zettenberg K, Siegbahn P. *Organometallics* 1997;16:1933.
- [35] Froese RDJ, Musaev DG, Matsubara J, Morokuma K. *J Am Chem Soc* 1997;119:7190.
- [36] Musaev DG, Froese RDJ, Morokuma K. *New J Chem* 1997;22:1269.
- [37] Froese RDJ, Musaev DG, Morokuma K. *J Am Chem Soc* 1998;120:1581.
- [38] Froese RDJ, Musaev DG, Morokuma K. *Organometallics* 1998;17:1850.
- [39] Deng L, Margl P, Ziegler T. *J Am Chem Soc* 1997;119:1094.
- [40] Froese RDJ, Musaev DG, Morokuma K. *Organometallics* 1999;18:373.
- [41] Deng L, Margl P, Ziegler T. *J Am Chem Soc* 1999;121:6479.
- [42] Margl P, Deng L, Ziegler T. *Organometallics* 1998;17:933.
- [43] Margl P, Deng L, Ziegler T. *J Am Chem Soc* 1998;120:5517.
- [44] Margl P, Deng L, Ziegler T. *J Am Chem Soc* 1999;121:154.
- [45] Allen FH, Davies JE, Galloy JJ, Johnson O, Kennard O, Macrae CF, Mitchell EM, Mitchell GF, Smith JM, Watson DG. *J Chem Inf Comput Sci* 1991;31:187.
- [46] Baerends EJ, Bérces A, Bo C, Boerrigter PM, Cavallo L, Deng L, Dickson RM, Ellis DE, Fan L, Fischer TH, Fonseca Guerra C, van Gisbergen SJA., Groeneveld JA, Gritsenko OV, Harris FE, van den Hoek P, Jacobsen H, van Kessel G, Kootstra F, van Lenthe E, Osinga VP, Philipsen PHT, Post D, Pye CC, Ravenek W, Ros P, Schipper PRT, Schreckenbach G, Snijders JG, Sola M, Swerhone D, te Velde G, Vernooijs P, Versluis L, Visser O, van Wezenbeek E, Wiesenekker G, Wolff SK, Woo TK, Ziegler T. *ADF* 1999.02
- [47] Fonseca Guerra C, Snijders JG, te Velde G, Baerends EJ. *Theor Chem Acc* 1998;99:391.
- [48] *ADF user's guide*. ADF Program System Release 1999.02
- [49] Hay PJ, Wadt WR. *J Chem Phys* 1985;82:270.
- [50] Wadt WR, Hay PJ. *J Chem Phys* 1985;82:284.
- [51] Hay PJ, Wadt WR. *J Chem Phys* 1985;82:299.
- [52] Vosko H, Wilk L, Nusair M. *Can J Phys* 1980;58:1200.
- [53] Becke AD. *Phys Rev A* 1988;38:3098.
- [54] Perdew JP. *Phys Rev B* 1986;33(12):8822.
- [55] Hehre WJ, Lou L. *A guide to density functional calculation in Spartan*. Irvine, CA: Wavefunction, Inc, 1997.
- [56] Arlman EJ, Cossee P. *J Catal* 1964;3:99.
- [57] Brookhart M, Green MLH. *J Organomet Chem* 1983;250:395.

<sup>1</sup> Following the referee's comments and in order to elucidate the effect of polarisation functions, extra-calculations using an augmented basis set with polarisation functions have been performed. The new basis set was a double-zeta basis set augmented with a simple polarisation function of d-type for the elements from Li to Xe [55]. These calculations have been performed over the sim.1a and sim.1b systems. The principal results are: (a) the geometries calculated by both basis sets are similar with the differences being smaller than 0.1 Å in distances and 1° in angles, (b) in terms of energies the difference between the energy barrier calculated by any of the two methods (basis set) is smaller than 2 kcal/mol. The calculated results are not much sensitive to the polarisation functions as the basis set with and without polarisation function provides similar results. These findings are consistent with other results from literature [38].